

Approved for public release;
distribution is unlimited.

Title:

PHYSICAL MECHANISMS OF IMPORTANCE TO
LASER THROMBOLYSIS

CONF-980117--

RECEIVED

MAY 28 1998

OSTI

Author(s):

Edward J. Chapyak and Robert P. Godwin,
Applied Theoretical and Computational
Physics Division,
Los Alamos National Laboratory,
Los Alamos, NM 87545

Submitted to:

Diagnostic and Therapeutic
Cardiovascular Interventions VIII
Conference Chair: Kenton W. Gregory, MD

Proceedings
BiOS'98, An International Symposium on
Biomedical Optics
24-30 January 1998
San Jose Convention Center, San Jose, CA
SPIE Code Number: 3245A-01

DISTRIBUTION OF THIS DOCUMENT IS UNLIMITED

MASTER

Los Alamos
NATIONAL LABORATORY

Los Alamos National Laboratory, an affirmative action/equal opportunity employer, is operated by the University of California for the U.S. Department of Energy under contract W-7405-ENG-36. By acceptance of this article, the publisher recognizes that the U.S. Government retains a nonexclusive, royalty-free license to publish or reproduce the published form of this contribution, or to allow others to do so, for U.S. Government purposes. Los Alamos National Laboratory requests that the publisher identify this article as work performed under the auspices of the U.S. Department of Energy. The Los Alamos National Laboratory strongly supports academic freedom and a researcher's right to publish; as an institution, however, the Laboratory does not endorse the viewpoint of a publication or guarantee its technical correctness.

DISCLAIMER

This report was prepared as an account of work sponsored by an agency of the United States Government. Neither the United States Government nor any agency thereof, nor any of their employees, makes any warranty, express or implied, or assumes any legal liability or responsibility for the accuracy, completeness, or usefulness of any information, apparatus, product, or process disclosed, or represents that its use would not infringe privately owned rights. Reference herein to any specific commercial product, process, or service by trade name, trademark, manufacturer, or otherwise does not necessarily constitute or imply its endorsement, recommendation, or favoring by the United States Government or any agency thereof. The views and opinions of authors expressed herein do not necessarily state or reflect those of the United States Government or any agency thereof.

DISCLAIMER

Portions of this document may be illegible in electronic image products. Images are produced from the best available original document.

Physical Mechanisms of Importance to Laser Thrombolysis

E. J. Chapyak and R. P. Godwin

Applied Theoretical and Computational Physics Division
Los Alamos National Laboratory
Los Alamos, New Mexico 87545

ABSTRACT

Bubble dynamics plays a key role in many medical procedures including Laser Thrombolysis (L-T), acoustic and laser lithotripsy, interocular laser surgery, photoacoustic drug delivery, and perhaps ultrasonic imaging. We are investigating the effect that interfaces of different materials, especially biological and biomedical materials, have on the dynamics of nearby bubbles. Collapsing bubbles often become nonspherical, resulting in spectacular directed motion with potentially both beneficial and undesirable consequences. This directed motion may explain L-T mass removal and some types of laser-induced tissue damage.

Keywords: laser thrombolysis, bubble dynamics, numerical methods, hydrodynamics, material properties, tissue properties

1. INTRODUCTION

For the past few years, the Oregon Medical Laser Center (OMLC) has conducted laser energy deposition experiments with gelatin thrombus surrogates.¹⁻³ These experiments have generally consisted of gelatin and a fluid in planar contact. A thin layer of gelatin, directly below the fluid, is impregnated with a dye that mimics the photo absorption characteristic of thrombus. An optical fiber positioned in the fluid above the interface delivers laser energy that is transmitted through the intervening fluid and absorbed in the colored gelatin. Bubble growth and collapse is always observed near the interface, provided that the energy in the laser pulse is sufficiently large. Interpenetration of the interface, accompanied by significant gelatin mass removal, also is observed at late time.

Figure 1 shows a sequence of nominally identical OMLC experiments, each one photographed at a different time. Here, a 577 nm dye laser delivers 50 mJ of energy in approximately 1 μ s through an optical fiber, about 0.33 mm in diameter, terminated 1 mm above a gelatin-water interface. The dye layer in the 175 bloom gelatin is 1 mm thick and has an absorption coefficient of 250 cm^{-1} . These experiments are confined within a cuvette of 1 cm by 1 cm square cross section. The gelatin layer in the cuvette is 4 cm thick and is covered with about 2 cm of water, above which is air at atmospheric pressure.

Our efforts at understanding these experimental results have focused on investigating the dynamics of collapsing bubbles near the gelatin-overfluid interface. Because of the highly distorted nonspherical flows that evolve, numerical simulations with the MESA-2D Eulerian computer code in cylindrical geometry have served as our primary analysis tool. (MESA-2D has been benchmarked against several bubble dynamics problems.³⁻⁵) In these studies, we have modeled the gelatin as water with slightly altered material properties. To date, we have considered two gelatin models; water with an enhanced viscosity, and water with a low elastic-plastic material strength.

Reference 3 discusses the implications of the "viscous water" gelatin model when water is the overfluid. In this paper, we present the implications of the second gelatin model with several overfluids. The results presented in Ref. 3 suggest that a collapsing bubble at the gelatin-water interface produces a well-defined jet of water that penetrates the gelatin. Although this behavior is not observed in the OMLC experiments, where gelatin penetrates into the water, it nevertheless suggests that interpenetrating flows can be generated from bubble collapse near an interface between materials with only slight differences in material properties.

2. OVERFLUID DENSITY VARIATIONS

Clinical applications of L-T employ a contrast agent, which is delivered through the catheter encapsulating the fiber optic. The contrast agent displaces the arterial blood near the thrombus. Moreover, properties of this contrast agent can be modified easily by dilution with saline solution. Thus, there is considerable interest in characterizing L-T mass removal with different overfluids. The OMLC surrogate experiments have explored this parameter space by utilizing undiluted contrast

fluid, which has a somewhat higher density than water (~1.4 g/cc), and mineral oils, which have lower densities (~0.8 g/cc), as overluids.

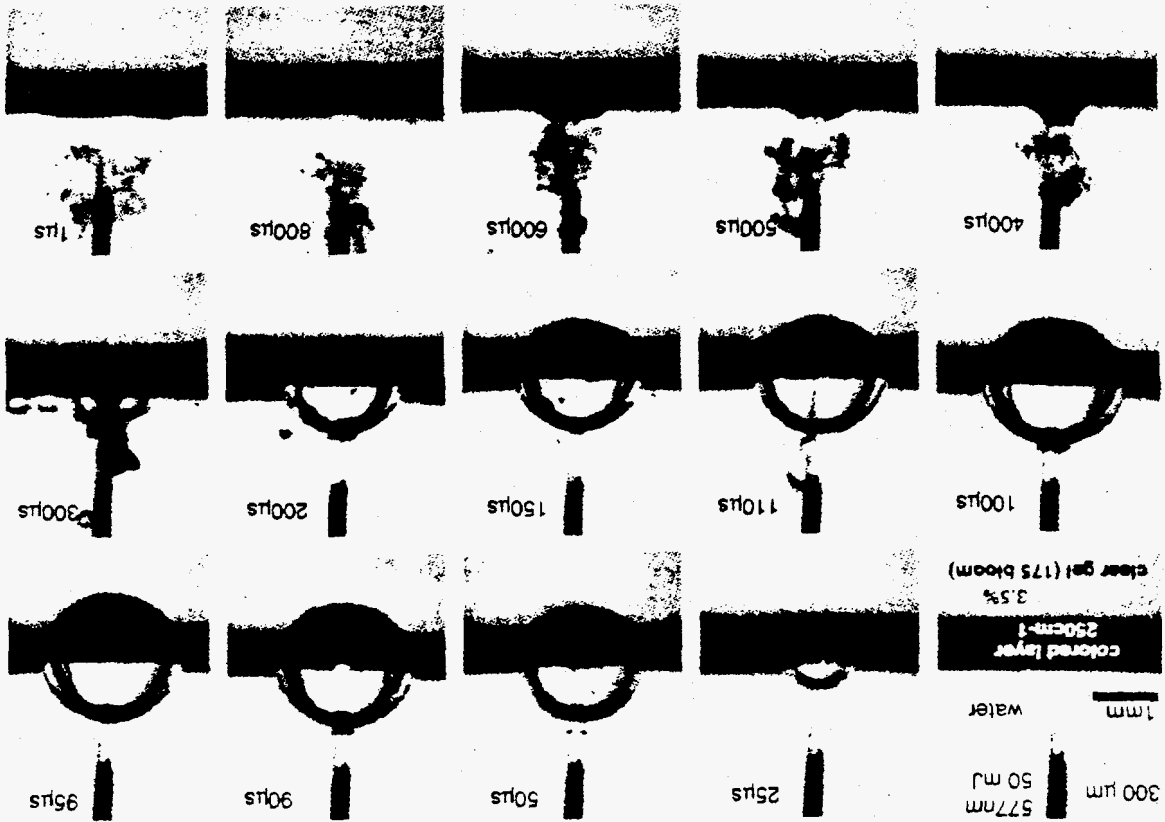


Fig. 1. OMLC laser deposition experimental time sequence.

We investigated the effect of overluid density by performing MESA-2D numerical simulations of the OMLC experimental geometry. In order to isolate density variations from other material property differences, we replaced the clot surrogate with water modeled with a Mie-Grunisen⁶ equation-of-state. Two overluid models were investigated: a Mie-Grunisen water with the initial density adjusted to 1.4 g/cc, and a Mie-Grunisen water with the initial density at 0.8 g/cc. Thus, the first simulation has 1.4 g/cc "water" over nominal water, while the second simulation has 0.8 g/cc "water" over nominal water. The same high pressure, spherical "seed" bubble as employed in Ref. 3 is used to initiate bubble growth. We believe that the interpenetrating flows that develop at late time should be rather insensitive to how bubble growth is initiated as long as the maximum bubble size is comparable to those observed in the laser experiments and large compared to the region of laser deposition.

Figure 2 shows bubble wall position for the high density simulation at different times during expansion (left), collapse (center), and at late time (right), where the numbers indicate time in μ s. The optical fiber appears as the cylindrical object projecting from the top. The right hand axis in all plots is an axis of cylindrical symmetry. The most dramatic feature apparent in Fig. 1 is the prominent water that penetrates into the 1.4 g/cc "water" overluid. Figure 3 shows similar information for the low density simulation. The most dramatic feature apparent in Fig. 3 is the prominent jet of 0.8 g/cc "water" that penetrates into the nominal water below. We conclude that in layered fluid systems with density discontinuities, bubble growth and collapse at the interface of discontinuity leads to penetration of light fluid into heavy fluid in the next section, we provide an analysis that explains some of the more subtle features found in Figs. 2 and 3.

3. MOMENTUM CONSERVATION AND SIMILARITY

The equation of motion for continuum dynamics can be expressed in the integral form⁷

$$\frac{\partial}{\partial t} \int \rho v_i dV = - \oint \Pi_{ik} dS_k, \quad (1)$$

where Π_{ik} , the momentum flux tensor, is given by

$$\Pi_{ik} = -\sigma_{ik} + \rho v_i v_k,$$

with v_i the velocity, ρ the density, and σ_{ik} the stress tensor of the continuum. For viscous fluids one can usually choose a surface distant enough from the bubble center such that the right hand side of Eq. 1 is quite small. Under these conditions

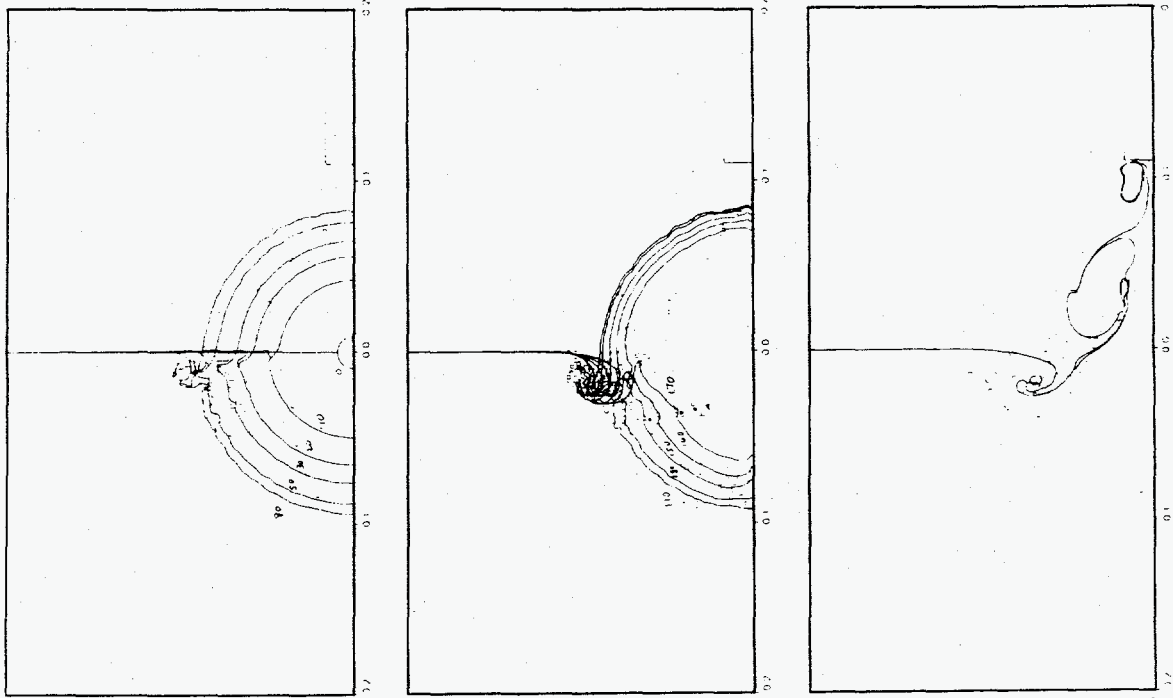


Fig. 2. Bubble interface time sequence for 1.4 g/cc "water" over nominal water.

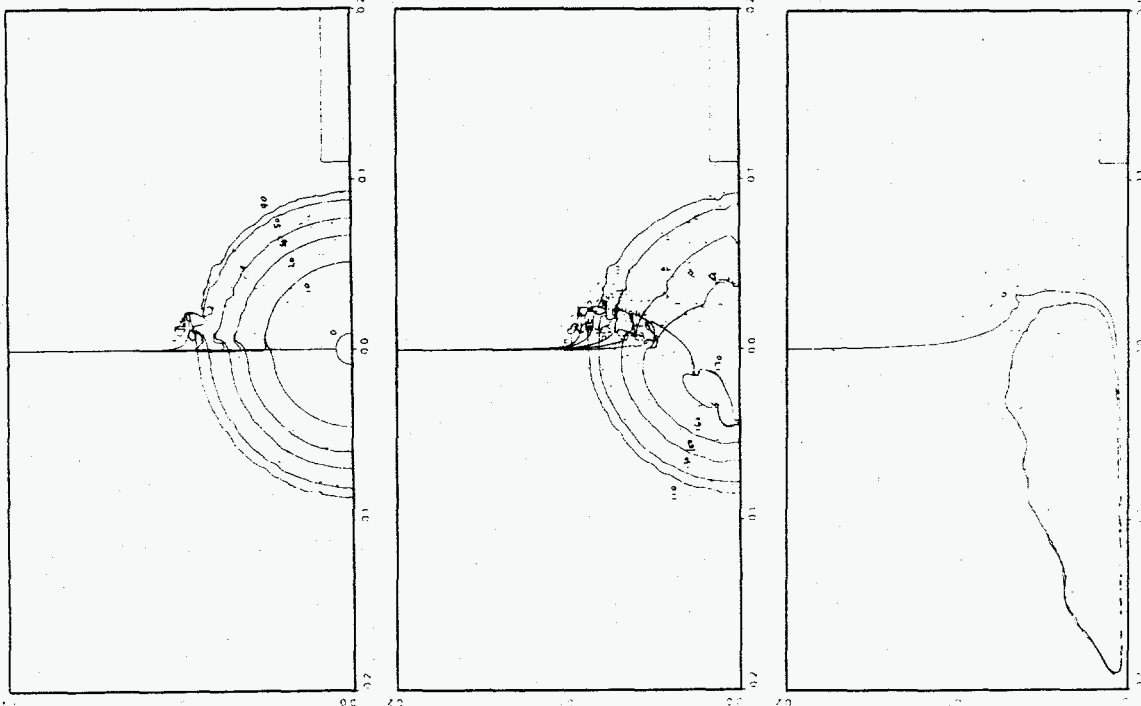


Fig. 3. Bubble interface time sequence for 0.8 g/cc "water" over nominal water.

$$\frac{\partial}{\partial t} \int \rho v_i dV \equiv 0,$$

and momentum approximately is conserved over the volume enclosed by the surface.

A useful model for the density dominated problems discussed above is the "split-sphere" model, at least during bubble expansion and the early stages of the collapse phase. This model has the bubble consisting of two hemispheres, joined at the equator, with the radius-time behavior of each hemisphere governed by the Rayleigh-Plesset (R-P) Equation³ (neglecting viscosity and surface tension). A similarity analysis of the R-P Equation indicates that if $R(t)$ is the spherical bubble radius as a function of time with a surrounding $\rho = 1$ fluid, then $R(t/\sqrt{\rho})$ must be the bubble radius with a surrounding density ρ fluid. This implies, for example, that, at a particular time during bubble expansion, the bubble on the high-density-fluid side will be smaller than the bubble on the low-density-fluid side and that the collapse on the low-density side will lead the collapse on the high-density side, although the maximum bubble size on both sides will be the same. This is indeed the case in Figs. 2 and 3.

One can also show that the momentum density, which is proportional to $\rho(dR/dt)$ is greater on the high density side than on the low density side. This implies that the "split-sphere" has an imbalance of momentum that cannot persist if momentum is conserved. We believe that the "fingers" of heavy fluid penetrating into the light fluid at the bubble equator in Figs. 2 and 3 are nature's way of correcting the "split-sphere" model to conserve momentum.

4. GELATIN STRENGTH EFFECTS

Thrombus and the thrombus surrogates (gelatin) used in the OMLC experiments have a limited ability to support shear stresses. If we imagine straining a sample of gelatin, initially the stresses will grow proportional to the strains. This is referred as the elastic regime. After some amount of strain develops, the material begins to deform plastically, where stresses increase only slightly with large increases in strain. Plastic deformation is irreversible in the sense that the material does not return to its initial shape after stresses relax to zero.

The numerical simulations that follow use an elastic-perfectly plastic material strength representation for the gelatin. Once the plastic limit is reached in this model, strains increase without any increase in applied stresses. Two material constants are required to characterize this model. The first, elastic, parameter is the shear modulus of the material, denoted by μ . The second, plastic, parameter is the plastic flow stress, denoted by Y . Values of shear modulus for gelatin have been measured⁸ and typically are a few tenths of a bar. Plastic flow stress values for gelatin are less well known, but cannot be more than about 0.2 bar without implying larger top-to-bottom asymmetries than are observed in the OMLC experiments.

Figure 4 shows bubble interface position at various times for a simulation of gelatin ($\mu=0.4$ bar, $Y=0.1$ bar, otherwise nominal water properties) and an overfluid of nominal water. The convention in Fig. 4 follows that of Figs 2 and 3. Note the jet of gelatin that penetrates into the water and impacts the fiber optic at late time. This behavior is actually quite similar to that observed in the OMLC experiments (see Fig. 1), and the mass of gelatin in the simulated jet is comparable to measured values in the OMLC experiments whose bubbles reach a similar maximum size.⁹ These experiments also suggest that turbulent diffusion dilutes and mixes the gelatin jet with water at very late times. This effect is not modeled in our current simulations.

Additional simulations utilizing a range of gelatin strength parameters suggest that lowering the shear modulus somewhat strengthens the jetting effect (and conversely), and that raising the plastic flow stress increases top-bottom asymmetry.

5. COMBINED OVERFLUID DENSITY AND GELATIN STRENGTH EFFECTS

We conclude with some results on the combined effect of overfluid density and gelatin strength. Figure 5 shows bubble interface position at various times for a simulation with gelatin as modeled in the Fig. 4 problem, but with an overfluid of 1.4 g/cc density "water", the same overfluid as in the Fig. 2 problem and representative of undiluted contrast fluid. The bubble interfaces in Fig. 5 look similar to those of Fig 4, except that the jet produced at late time in Fig. 5 is somewhat larger than that in Fig. 4.

Figure 6 shows similar information for the same gelatin model, but with an overfluid of 0.8 g/cc "water", the same overfluid as considered in the Fig. 3 simulation. Here, the jet is suppressed and a film of gelatin is propelled into the overfluid. In this case, ejection of gelatin still may occur, but the mechanism is quite different from the jetting observed in previous simulations. These trends with overfluid density are qualitatively reasonable in view of the fluid behavior indicated in Figs. 2 and 3.

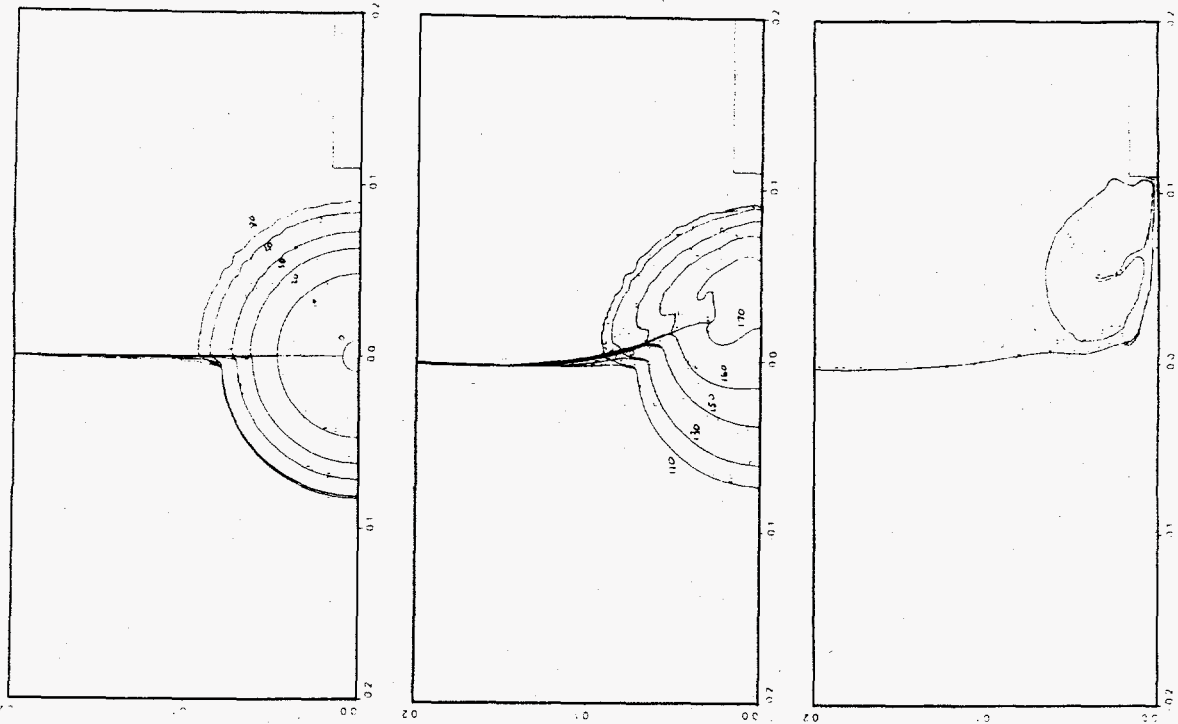


Fig. 4. Bubble interface time sequence for gelatin ($\mu=0.4$ bar, $Y=0.1$ bar, otherwise nominal water properties), below, nominal water, above.

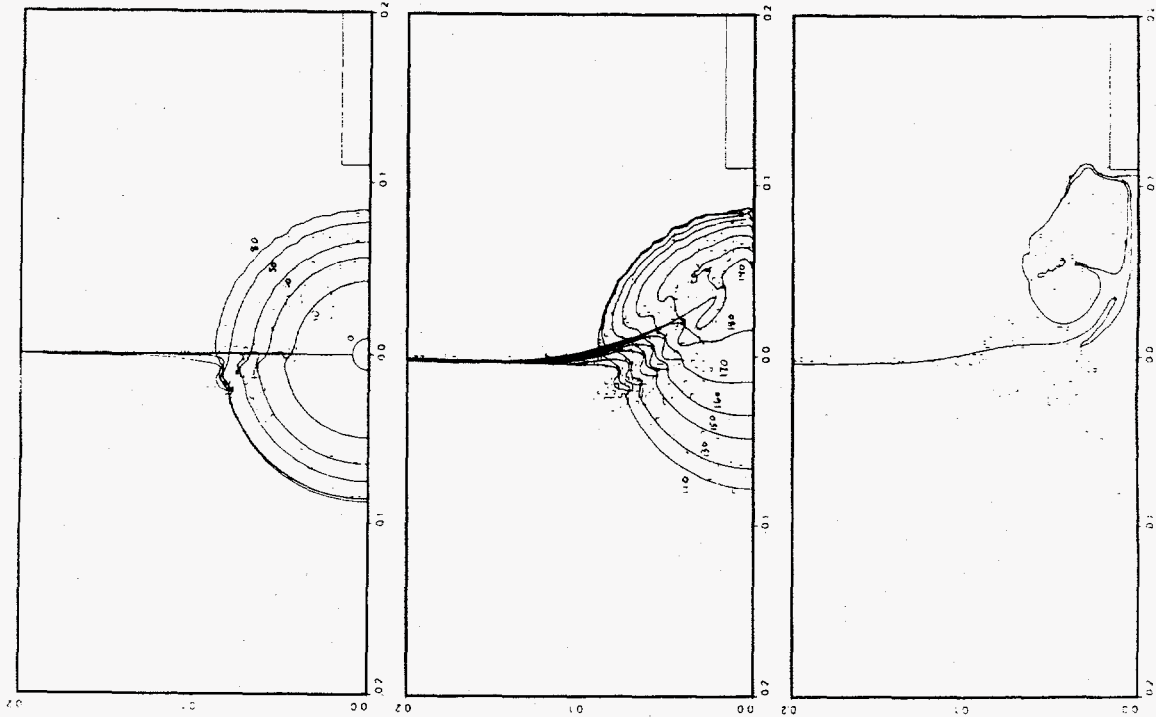


Fig. 5. Bubble interface time sequence for gelatin ($\mu=0.4$ bar, $Y=0.1$ bar, otherwise nominal water properties), below, 1.4 g/cc "water", above.

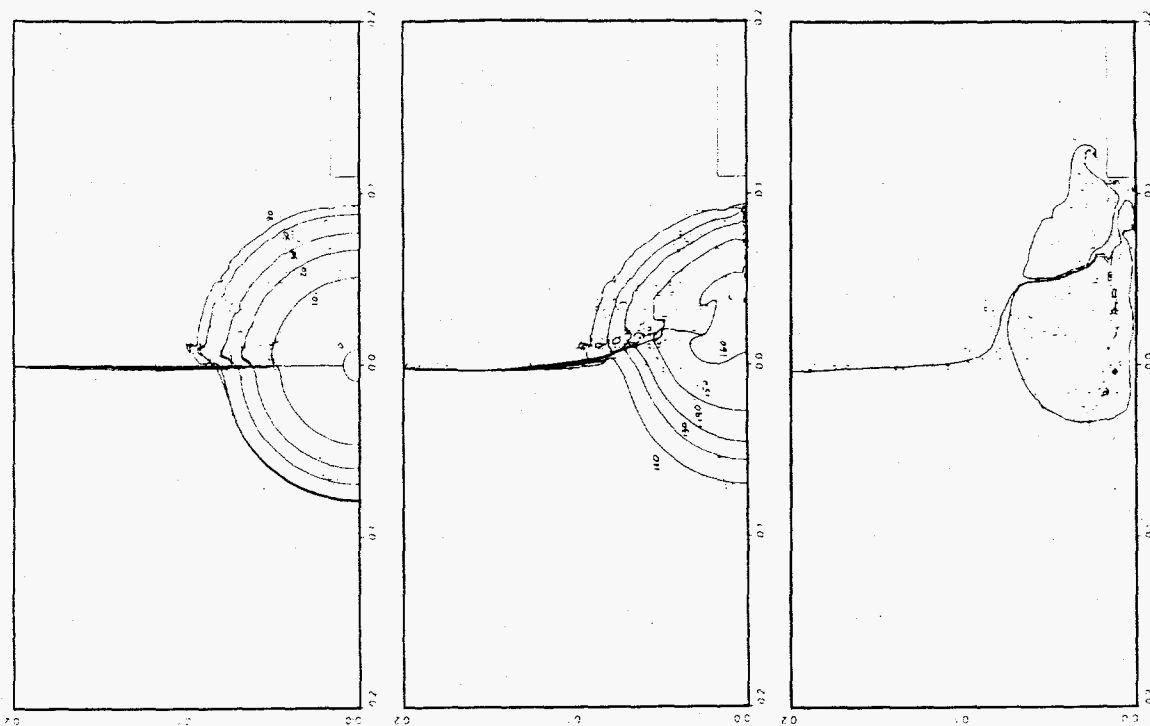


Fig. 6. Bubble interface time sequence for gelatin ($\mu=0.4$ bar, $Y=0.1$ bar, otherwise nominal water properties), below, 0.8 g/cc "water", above.

6. CONCLUSIONS

Interpenetrating flows generated by laser-initiated bubble growth and collapse near interfaces between different biological/ biomedical materials can explain some of the observed mass removal in Laser Thrombolysis as well as laser-induced tissue damage. Numerical simulations suggest that laser energy deposition at an interface between a) fluids of different density, but with the same viscosity, produces penetration of the heavier fluid by the lighter fluid, and b) fluids of different viscosity, but with the same density, produces penetration of the more viscous fluid by the less viscous fluid.

Interfaces between fluids and materials with strength produce more complex results, with penetration possible in either direction, depending on specific material property values. Simulations of the water-over-gelatin L-T experiments at the OMLC suggest that gelatin is ejected into the water when realistic strength model parameters are assigned to the gelatin, in qualitative agreement with the experimental observations.

7. ACKNOWLEDGMENTS

This work was supported in part by a Cooperative Research and Development Agreement (CRADA) between Los Alamos National Laboratory (Department of Energy), Oregon Medical Laser Center, and Palomar Medical Technologies.

8. REFERENCES

1. U. S. Sathyam, A. Shearin, E. A. Chastaney, and S. A. Pahl, "Threshold and ablation efficiency studies of microsecond ablation of gelatin under water," *Lasers Surg. Med.*, **19**, 397-406, 1996.
2. H. Shangguan, L. W. Casperson, and S. A. Pahl, "Microsecond Laser Ablation of Thrombus and Gelatin under Clear Liquids: Contact vs. Non-contact," *IEEE J. Selected Topics Quantum Electron.*, **2**, 818-825, 1996.
3. E. J. Chapyak, R. P. Godwin, S. A. Pahl, and H. Shangguan, "A Comparison of Numerical Simulations and Laboratory Studies of Laser Thrombolysis," *Lasers in Surgery: Advanced Characterization, Therapeutics, and Systems VII, Proc. SPIE*, **2970**, 28-34, 1997.

4. E. J. Chapyak and R. P. Godwin, "Numerical Studies of Bubble Dynamics in Laser Thrombolysis," *Lasers in Surgery: Advanced Characterization, Therapeutics, and Systems VI, Proc. SPIE*, 2671, 84, 1996.
5. E. J. Chapyak, R. P. Godwin, and A. Vogel, "A Comparison of Numerical Simulations and Laboratory Studies of Shock Waves and Cavitation Bubble Growth Produced by Optical Breakdown in Water," *Lasers in Surgery: Laser-Tissue Interaction VIII, Proc. SPIE* 2975, 335-342, 1997.
6. F. H. Harlow, and A. A. Amsden, "Fluid Mechanics," Los Alamos Scientific Laboratory Report LASL-4700, 1971.
7. L. D. Landau, and E. M. Lifshitz, *Fluid Mechanics*, p. 13, Pergamon Press, 1959.
8. J. K. Dienes, P. L. Coleman, M. Intaglietta, and J. E. Welch, "The Response of Gelatin to High Speed Impact," Systems, Science and Software report SSS-R-73-1891, 1973.
9. R. P. Godwin, E. J. Chapyak, S. A. Prahl, and H. Shangguan, "Laser Mass Ablation Efficiency Measurements Indicate Bubble-Driven Dynamics Dominates Laser Thrombolysis" *Lasers in Surgery: Advanced Characterization, Therapeutics, and Systems VIII, Proc SPIE*, 3245, 1998 (to be published).